The Spitzer Space Telescope: New Views of the Cosmos
ASP Conference Series, Vol. 357, 2006
L. Armus and W.T. Reach

Observations of Ultraluminous Infrared Galaxies with the IRS on Spitzer

L. Armus and the IRS GTO Team
Spitzer Science Center
California Institute of Technology

Abstract.
We present spectra taken with the Infrared Spectrograph on Spitzer covering the $5-38\mu$m region of the ten Ultraluminous Infrared Galaxies (ULIRGs) found in the IRAS Bright Galaxy Sample. Among the BGS ULIRGs, we find a factor of 50 spread in the spectral slope from $5.5-60\mu$m in the rest frame. There is evidence for water ice and hydrocarbon absorption (from $5.5-6.5\mu$m) in 7/10 BGS ULIRGs, as well as absorption features of C_2H_2 and HCN in four and possibly six of the 10 BGS ULIRGs, indicating shielded molecular clouds and a warm, dense ISM. We have detected [NeV] emission at 14.3μm and 24.3μm in three out of the 10 BGS ULIRGs. The AGN fractions implied by either the [NeV]/[NeII] or [OIV]/[NeII] line flux ratios (or their upper limits) are significantly lower than implied by the MIR slope or strength of the 6.2μm PAH EQW feature.

In order to adequately sample the local ULIRG population, we are obtaining mid-infrared spectra of a large number (> 100) of ULIRGs having $0.02 < z < 0.93$ with the Infrared Spectrograph (IRS) on Spitzer, as part of the IRS guaranteed time program. These sources are chosen primarily from the IRAS 1-Jy (Kim & Sanders 1998), 2-Jy (Strauss et al. 1992), and the FIRST/IRAS radio-far-IR sample of Stanford et al. (2000). Here, we discuss the IRS spectra of the ten ULIRGs in the IRAS Bright Galaxy Sample (Soifer, et al. 1987). The Bright Galaxy Sample (BGS) is a flux-limited, complete sample of all 324 galaxies with 60μm IRAS flux densities greater than 5.4 Jy in the IRAS Point Source catalog (1985). The ten ULIRGs in the BGS, in order of increasing redshift, are Arp 220 ($z = 0.0181$), Mrk 273 ($z = 0.0378$), UGC 5101 ($z = 0.0400$), Mrk 231 ($z = 0.0422$), IRAS 05189-2524 ($z = 0.0426$), IRAS 15250+3609 ($z = 0.0554$), IRAS 08572+3915 ($z = 0.0584$), IRAS 12112+0305 ($z = 0.0727$), IRAS 22491-1808 ($z = 0.0773$), and IRAS 14348-1447 ($z = 0.0827$).

1. Observations

The ULIRGs were observed in the two low-resolution ($64 < R < 128$; Short-Low and Long-Low or SL & LL) and two high-resolution ($R \sim 650$; Short-High and Long-High or SH & LH) IRS modules, using the Staring Mode Astronomical Observing Template (AOT). The galaxies were placed at the two nod positions for each of the IRS slits. High accuracy IRS blue peak-ups were performed on nearby 2MASS stars for seven of the ten BGS sources, before offsetting to the target galaxies. For IRAS 12112+0305, and IRAS 14348-1447, and IRAS 22491-1808 we performed high-accuracy IRS blue peak-ups on the nuclei themselves. IRAS 08572+3915, IRAS 12112+0305, and IRAS 14348-1447 have well-resolved

double nuclei (see Condon et al. 1990, Evans et al. 2000,2002). In the case of IRAS 08572+3915, the IRS observations were centered on the NW nucleus, which dominates the near and mid-infrared emission (Soifer et al. 2000). For IRAS 12112+0305 and IRAS 14348-1447, the slits were centered on the NE and SW nuclei, respectively.

2. Results

2.1. Continuum & Dust Features

Broad, emission features associated with Poly-cyclic Aromatic Hydrocarbons (PAHs) at 6.2, 7.7, 8.6, 11.3, and 12.7μm, along with absorption from amorphous silicates centered at 9.7 and 18μm dominate the spectra in nearly all cases. We also often detect the weaker PAH emission at 14.2, 16.4, 17.1μm, and 17.4μm. The broad 17.1μm feature sits under both the 16.4μm and 17.4μm PAH features (see Smith et al. 2004) and the H_2 S(1) line which is often prominent in the ULIRG spectra. There is a large range in spectral shape across the IRS wavelength range ($5 - 38\mu$m), among the sample galaxies. IRAS 05189-2524 and Mrk 231 have relatively flat spectra with weak silicate absorption and weak PAH emission. At the other extreme are sources like UGC 5101 and IRAS 14348-1447 which have very strong PAH emission, deep silicate absorption, and water ice (most easily seen as a strong absorption from $\sim 5.5 - 6.5\mu$m, under the 6.2μm PAH emission feature). Water ice absorption is also evident in Arp 220, Mrk 273, and IRAS 15250+3609, and is indicative of shielded molecular clouds along the line of sight to the ULIRG nuclei. Of the seven sources with detected PAH emission at 6.2μm, IRAS 15250+3609 has the weakest 6.2μm PAH equivalent width (only 0.022μm). For the BGS sample as a whole, the silicate optical depths range from $\tau_{9.7} \leq 0.43$ ($A_V \leq 7.9$ mag) in IRAS 05189-2524, to $\tau_{9.7} = 4.21$ ($A_V = 78$ mag) in IRAS 08572+3915, and $A_V/\tau_{9.7} = 18.5$ from Roche & Aitken (1984). IRAS 08572+3915 has the flattest (bluest), and Arp 220 has the steepest (reddest) spectrum of of the BGS ULIRG sample. There is nearly a factor of 50 (25) spread among the ULIRGs at 5.5μm when normalized at 60μm (25μm).

Fitting the SEDs, we see evidence for hot (T > 300K) dust in 5/10 of the BGS ULIRGs, namely UGC 5101, IRAS 05189-2524, Mrk 231, IRAS 08572+3915, and Arp 220. The fraction of hot dust to total dust luminosity is highest in IRAS 08572+3915 ($\sim$ 23%, before correcting for considerable extinction). The temperature of the hot dust is highest in UGC 5101 and Arp 220 (T $\sim$ 700K), but the fraction of the total luminosity is lowest in these sources, 8% and 1%, respectively. Mrk 463e, Mrk 1014 and NGC 6240 also show evidence for hot dust in their spectra.

We also detect absorption features from gas-phase interstellar C_2H_2 and HCN at 13.7μm and 14.0μm, respectively, in four of the ten BGS ULIRGs, namely Mrk 231, Arp 220, IRAS 08572+3915, and IRAS 15250+3609. Equivalent widths for the C_2H_2 and HCN absorption lines range from $0.002 - 0.012\mu$m, and $0.002 - 0.007\mu$m, respectively, with IRAS 15250+3609 having the deepest absorption.

2.2. Emission Lines

The high-resolution ULIRG spectra are dominated by unresolved atomic, fine-structure lines of Ne, O, Si, and S, covering a large range in ionization potential. Some features, e.g. the [NeV] lines at 14.3 and 24.3μm, imply the presence of an AGN by their very detection in a galaxy spectrum, since it takes 97.1 eV to ionize Ne^{3+}, and this is too large to be produced by O stars. Of the 10 BGS ULIRGs, we have detected [NeV] emission in three: IRAS 05189-2524, Mrk 273, and UGC 5101. The detection of [NeV] in UGC 5101 has been previously reported by Armus et al. (2004). The fluxes in the 14.32μm lines are 18.36, 12.86, and 5.10×10^{-14} erg cm^{-2} s^{-1}, in IRAS 05189, Mrk 273, and UGC 5101, respectively. In all three galaxies we detect both the 14.32μm and 24.32μm [NeV] lines. The nearby, low-ionization [ClII] feature at 14.37μm can easily be mistaken for [NeV], but the resolution of the IRS and the high S/N of our data allow us to separate out the two lines in all cases. We have detected the [ClII] line in 5/10 of the BGS ULIRGs. In some cases, such as Mrk 273, both the [NeV] and the [ClII] lines are detected. In others, such as Arp 220, only the [ClII] line is seen.

Constructing excitation diagrams from the [NeV]/[NeII], [OIV]/[NeII] and 6.2μm PAH equivalent width (EQW) suggests that Mrk 463e, Mrk 1014, and IRAS 05189-2524 are AGN dominated, while IRAS 12112+0305, IRAS 14348-1447, IRAS 22491-1808, and Arp 220 are starburst-dominated. Mrk 273 appears to have a significant starburst contribution $(30 - 50\%)$ to it's total luminosity. Mrk 231, IRAS 08572+3915, and IRAS 15250+3609 show very weak 6.2μm PAH emission, and yet are undetected in [NeV] or [OIV], even though they are optically classified as a Seyfert 1 (Mrk 231), and LINERs (IRAS 08572+3915 and IRAS 15250+3609), respectively. Two sources, UGC 5101 and NGC 6240 have very weak [NeV] and hot dust emission, indicative of buried AGN. This is supported by the fact that both of these sources have significant hard x-ray emission behind extremely large columns of HI ($1-2\times10^{24}$ cm^{-2}). In all ULIRGs in this study, except for Mrk 463 and Mrk 1014, the AGN fractions implied by either the [NeV]/[NeII] or [OIV]/[NeII] line flux ratios (or their upper limits) are significantly lower than implied by the MIR slope or strength of the 6.2μm PAH EQW feature. We find evidence for AGN in the mid-infrared spectra of ULIRGs with optical/NIR Seyfert or LINER classifications. We do not find evidence for buried AGN in ULIRGs classified optically as starburst-like among the BGS sample. However, the AGN fractions implied by the [NeV]/[NeII] or [OIV]/[NeII] line flux ratios are often significantly lower than suggested by either the mid-infrared slope or the strength of the 6.2μm PAH feature.

References

Armus, L. et al. 2004, ApJS, 154, 178.
Armus, L., et al. 2006, ApJ, 640, 204.
Brandl, B.R., et al. 2006, ApJ, in press.
Genzel, R., Lutz, D., Sturm, E., Egami, E., Kunze, D., et al. 1998, ApJ, 498, 589.
Kim, D.C., & Sanders, D.B. 1998, ApJS, 119, 41.
Smith, J.D.T., et al. 2004, ApJ Suppl., 154, 199.
Soifer, B.T., et al. 1987, ApJ, 320, 238.
Soifer, B.T., et al. 2000, AJ, 119, 509.

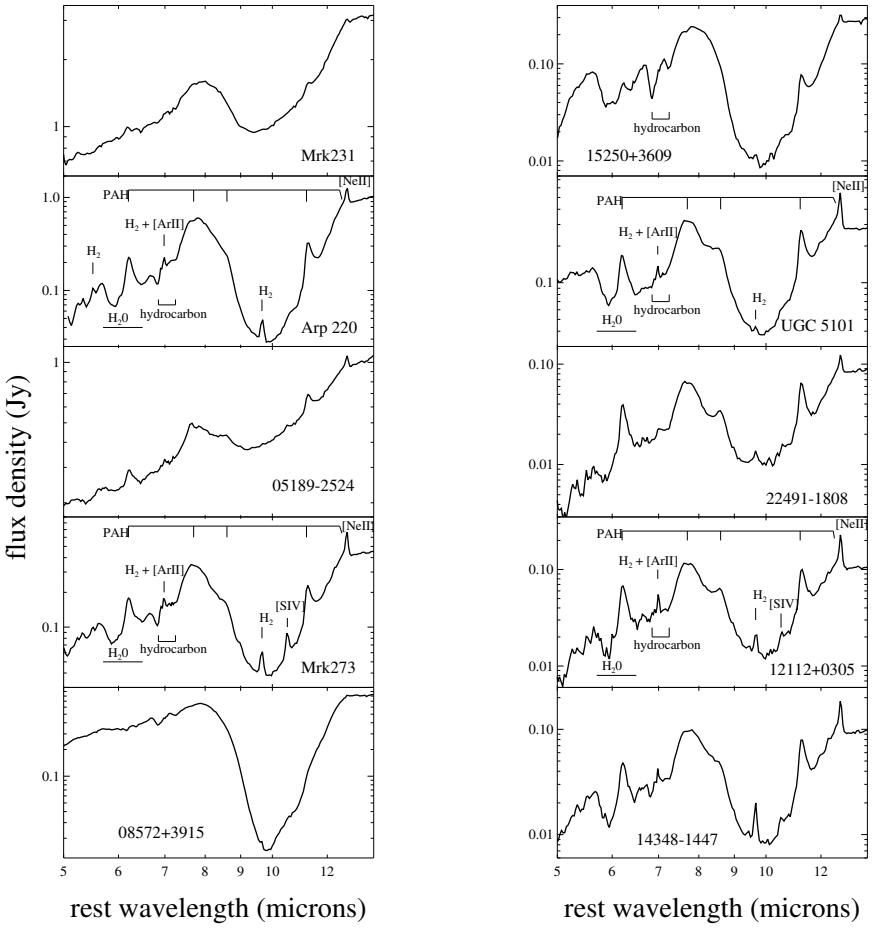

Figure 1. IRS Short-Low spectra of the 10 BGS ULIRGs. Prominent emission features and absorption bands (the latter indicated by horizontal bars) are marked on representative spectra in each sub-panel.

Spoon, H.W.W., Keane, J.V., Tielens, A.G.G.M., Lutz, D., Moorwood, A.F.M., & Laurent, O. 2002, A & A, 385, 1022.
Spoon, H.W.W., et al. 2004, ApJ Suppl., 154, 184.
Stanford, S.A., Stern, D., van Breugel, W., & De Breuck, C. 2000, ApJ Suppl., 131, 185.
Strauss, M.A., Huchra, J.P., Davis, M., Yahil, A., Fisher, K.B., & Tonry, J. 1992, ApJS, 83, 29.
Sturm, E., et al. 2002, A & A, 393, 821.
Weedman, D.W., et al. 2005, ApJ, 633, 706.

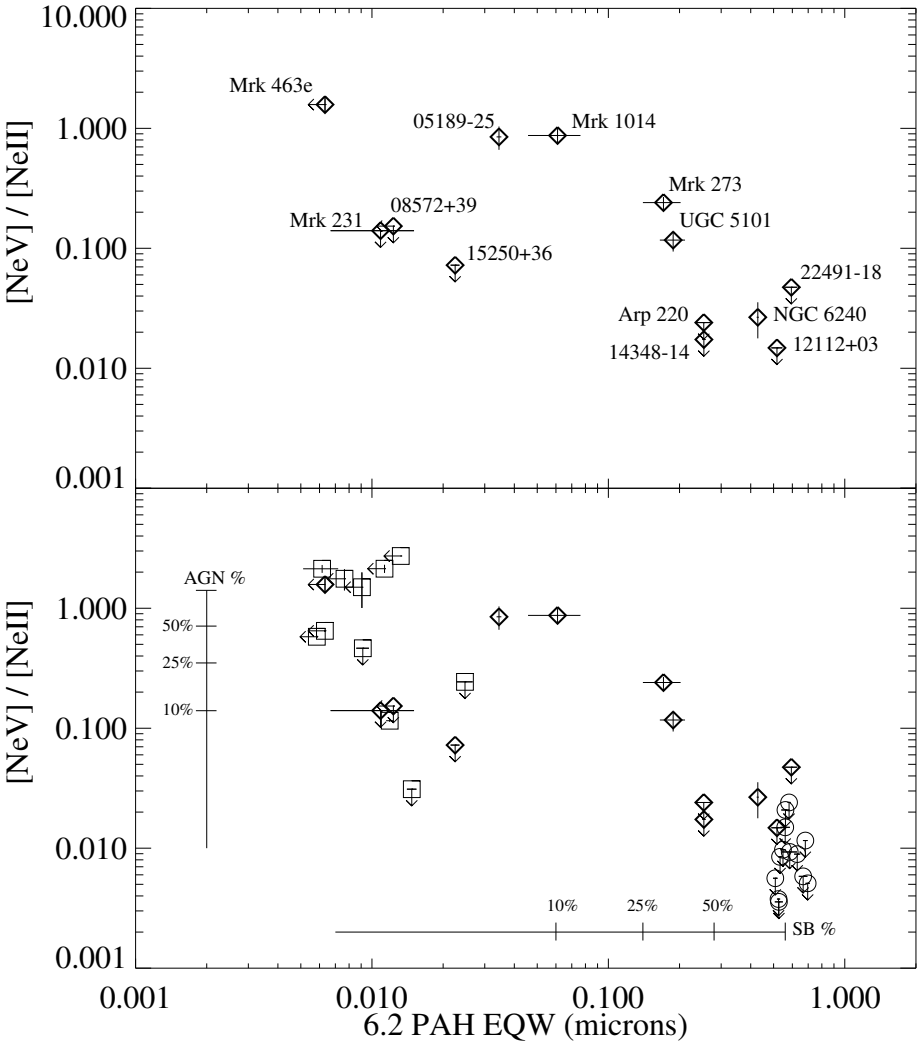

Figure 2. Mid-Infrared [NeV] excitation diagram for the BGS ULIRGs. The [NeV] 14.3/[NeII] 12.8 vs. 6.2 PAH EQW (Fig. 5a) for the 10 BGS ULIRGs (diamonds), together with a sample of AGN (squares - from Weedman et al. 2005) and starburst galaxies (circles - from Brandl et al. 2006). Also plotted are the ULIRGs Mrk 1014 and Mrk 463e (from Armus et al. 2004) and NGC 6240 (from Armus et al. 2006). The upper panel shows only the ULIRGs (labelled) while the lower panel shows the ULIRGs together with the AGN and Starburst galaxies. In all cases, one-sigma error bars and upper limits are indicated. The vertical and horizontal lines indicate the fractional AGN and starburst contributions to the [NeV]/[NeII] and 6.2μm PAH EQW, respectively, assuming a simple linear mixing model (e.g. Sturm et al. 2002). In each case, the 50%, 25% and 10% levels are marked. The 100% level is set by the average detected values for the [NeV]/[NeII] and 6.2μm EQW among the AGN and starbursts, respectively